

# A guide to super-resolution fluorescence microscopy

Lothar Schermelleh,<sup>1</sup> Rainer Heintzmann,<sup>2,3,4</sup> and Heinrich Leonhardt<sup>1</sup>

<sup>1</sup>Department of Biology and Center for Integrated Protein Science, Ludwig Maximilians University Munich, 82152 Planegg-Martinsried, Germany

<sup>2</sup>King's College London, Randall Division of Cell and Molecular Biophysics, New Hunt's House, Guy's Campus, London SE1 1UL, England, UK

<sup>3</sup>Institute of Physical Chemistry, Friedrich-Schiller University Jena, 07743 Jena, Germany

<sup>4</sup>Institute of Photonic Technology, 07745 Jena, Germany

For centuries, cell biology has been based on light microscopy and at the same time been limited by its optical resolution. However, several new technologies have been developed recently that bypass this limit. These new super-resolution technologies are either based on tailored illumination, nonlinear fluorophore responses, or the precise localization of single molecules. Overall, these new approaches have created unprecedented new possibilities to investigate the structure and function of cells.

## Introduction

The understanding of cellular functions requires detailed knowledge of all factors, their interactions and modifications as well as their distribution in the cell and dynamic changes thereof. From the very beginning, microscopy has played a key role in cell biology. Since the first studies of biological structures by early pioneers of microscopy like Robert Hooke and Antoni van Leeuwenhoek in the 17th century, technical developments and improved manufacturing have led to greatly improved image quality but were ultimately faced with a limit in optical resolution. Based on experimental evidence and basic principles of physics, Ernst Abbe and Lord Rayleigh defined and formulated this diffraction-limited resolution in the late 19th century (Abbe, 1873; Rayleigh, 1896). Later key innovations—including fluorescence and confocal laser scanning microscopy (CLSM)—made optical microscopy one of the most powerful and versatile diagnostic tools in modern cell biology. Using highly specific fluorescent labeling techniques such as immunocytochemistry, *in situ* hybridization, or fluorescent protein tags, the spatial distribution and dynamics

of virtually every subcellular structure, protein, or genomic sequence of interest can be analyzed in chemically fixed or living samples (Conchello and Lichtman, 2005; Giepmans et al., 2006).

Still, even with perfect lenses, optimal alignment, and large numerical apertures, the optical resolution of light microscopy was limited to approximately half of the wavelength of the light used. In practical terms this meant that only cellular structure and objects that were at least 200 to 350 nm apart could be resolved by light microscopy (see box for details). Much of the fundamental biology of the cell, however, occurs at the level of macromolecular complexes in the size range of tens to few hundred nm, i.e., beyond the reach of conventional light microscopy.

An early and powerful approach to obtain more detailed information is using electrons instead of photons. Following the same physical principal, but with a  $10^5$  times smaller wavelength, electron microscopy (EM) is able to achieve up to  $100\times$  greater resolving power. However, state-of-the-art transmission and scanning EM techniques are technically demanding, relatively costly, and time-consuming. Importantly, due to principles of signal detection, the possibility to specifically label and visualize multiple cellular structures or components in one specimen is still limited. Moreover, chemical fixation and contrasting procedures and/or physical sectioning render specimens vulnerable to artifacts and exclude the option to observe living cells or organisms at high resolution in their unperturbed state. Therefore, improving the resolution of fluorescence light microscopy while keeping its major advantages remains a pivotal challenge.

## Classical ways to enhance the resolution of light microscopy

The practically achieved resolution depends on many factors and reaches the theoretical limit only under optimal conditions. The best possible resolution as defined by the diffraction barrier can only be achieved in an environment with homogeneous refractive index, high signal intensity, and minimal background signals. In reality, optical aberrations and out-of-focus blur affect the signal-to-noise ratio and decrease the effectively achievable resolution, especially in the case of complex biological samples.

Correspondence to: Lothar Schermelleh: [lothar.schermelleh@lmu.de](mailto:lothar.schermelleh@lmu.de); Rainer Heintzmann: [heintzmann@gmail.com](mailto:heintzmann@gmail.com); or Heinrich Leonhardt: [h.leonhardt@lmu.de](mailto:h.leonhardt@lmu.de)

Abbreviations used in this paper: 3D-SIM, three-dimensional SIM; APD, avalanche photodiode; CCD, charge-coupled device; CLSM, confocal laser scanning microscopy; CMOS, complementary metal oxide semiconductor; CW-STED, continuous-wave STED; FPALM, fluorescence photoactivation localization microscopy; PALM, photoactivated localization microscopy; PMT, photomultiplier tube; PSF, point-spread-function; SSIM, saturated SIM; STED, stimulated emission depletion; STORM, stochastic optical reconstruction microscopy; SIM, structured illumination microscopy; TIRF, total internal reflection of fluorescence.

© 2010 Schermelleh et al. This article is distributed under the terms of an Attribution–Noncommercial–Share Alike–No Mirror Sites license for the first six months after the publication date (see <http://www.rupress.org/terms>). After six months it is available under a Creative Commons License (Attribution–Noncommercial–Share Alike 3.0 Unported license, as described at <http://creativecommons.org/licenses/by-nc-sa/3.0/>).

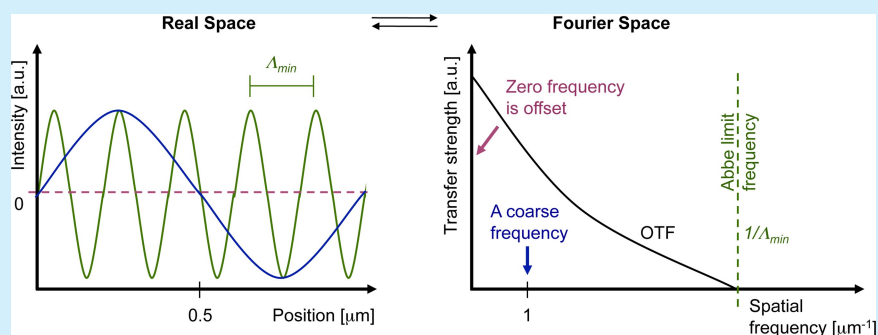
## Point spread function and the significance of convolution

The process of fluorescence imaging with a well-designed microscope is somewhat similar to painting the perfect object structure with a fuzzy brush. The shape (or rather the intensity distribution) of this brush is called the point spread function (PSF) as it describes how a point-like object is spread out in the image. The process of painting with such a fuzzy brush is mathematically called a convolution operation (object is convolved with PSF to form the image). Thus, the fineness as well as the shape of the brush (PSF) determines the level of detail that can be discerned in an image.

## The diffraction (Abbe) limit of detection

Resolution is often defined as the largest distance at which the image of two point-like objects seems to amalgamate. Thus, most resolution criteria (Rayleigh limit, Sparrow limit, full width at half maximum of the PSF) directly relate to properties of the PSF. These are useful resolution criteria for visible observation of specimen, but there are several shortcomings of such a definition of resolution: (1) Knowing that the image is an image of two particles, these can in fact be discriminated with the help of a computer down to arbitrary smaller distances. Determining the positions of two adjacent particles thus becomes a question of experimental precision and most notably photon statistics rather than being described by the Rayleigh limit. (2) These limits do not necessarily correspond well to what level of detail can be seen in images or real world objects; e.g., the Rayleigh limit is defined as the distance from the center to the first minimum of the point spread function, which can be made arbitrarily small with the help of ordinary linear optics (e.g., Toraldo-filters), albeit at the expense of the side lobes becoming much higher than the central maximum. (3) They are not motivated by the understanding that light is a diffracting wave which poses a finite limit to the level of detail contained in such waves, as explained below.

Abbe's formulation of a resolution limit avoids all of the above shortcomings at the expense of a less direct interpretation. The process of imaging can be described by a convolution operation. With the help of a Fourier transformation, every object (whether periodic or not) can uniquely be described as a sum of sinusoidal curves with different spatial frequencies (where higher frequencies represent fine object details and lower frequencies represent coarse details). The rather complex process of convolution can be greatly simplified by looking at the equivalent operation in Fourier space: The Fourier-transformed object just needs to be multiplied with the Fourier-transformed PSF to yield the



Fourier-transformed ideal image (without the noise). Because the Fourier-transformed PSF now describes how well each spatial frequency of the Fourier-transformed object gets transferred to appear in the image, this Fourier-transformed PSF is called the optical transfer function, OTF (right panel). Its strength at each spatial frequency (e.g., measured in oscillations per meter) conveniently describes the contrast that a sinusoidal object would achieve in an image.

Interestingly, the detection OTF of a microscope has a fixed frequency border (Abbe limit frequency, right panel). The maximum-to-maximum distance  $\Delta_{\min}$  of the corresponding sine curve is commonly referred to as Abbe's limit (left panel). In other words: The Abbe limit is the smallest periodicity in a structure, which can be discriminated in its image. As a point object contains all spatial frequencies, this Abbe limit sine curve needs to also be present in the PSF. A standard wide-field microscope creates an image of a point object (e.g., an emitting molecule) by capturing the light from that molecule at various places of the objective lens, and processing it with further lenses to then interfere at the image plane. Conveniently due to the reciprocity principle in optics, the Abbe limit  $\Delta_{\min}$  along an in-plane direction in fluorescence imaging corresponds to the maximum-to-maximum distance of the intensity structure one would get by interfering two waves at extreme angles captured by the objective lens:

$$\Delta_{\min} = \frac{\lambda}{2n \sin(\alpha)} = \frac{\lambda}{2NA},$$

where  $\lambda/n$  is the wavelength of light in the medium of refractive index  $n$ . The term  $NA = n \sin(\alpha)$  conveniently combines the half opening angle  $\alpha$  of the objective and the refractive index  $n$  of the embedding medium.

Abbe's famous resolution limit is so attractive because it simply depends on the maximal relative angle between different waves leaving the object and being captured by the objective lens to be sent to the image. It describes the smallest level of detail that can possibly be imaged with this PSF "brush". No periodic object detail smaller than this shortest wavelength can possibly be transferred to the image.

A widely used strategy to increase signal-to-noise ratio and thereby improve image resolution is the deconvolution of wide-field image z-stacks. This computational post-processing tries to reconstruct the most probable object, which could have given rise to the detected image by using the image of a point-like object—the point-spread-function (PSF, see box). This PSF is ideally determined experimentally for the particular microscope in use. Computational image restoration assigns out-of-focus intensity back to its originating position in space, resulting in a significantly improved image contrast and a modest increase in spatial resolution (Agard and Sedat, 1983; Agard et al., 1989; Wallace et al., 2001). Additional prior knowledge, such as the emitted signal being positive, enables deconvolution algorithms to "guess" details beyond Abbe's limit. However, the obtained improvement depends on the studied object with best results for sparse objects such as filaments or vesicles (Heintzmann, 2007) and little improvement for other objects.

Confocal laser scanning microscopy, in contrast, employs a redesigned optical path and specialized hardware. Here, a tightly focused spot of laser light is used to scan the sample and a small aperture (or pinhole) in the confocal image plane of the light path allows only light originating from the nominal focus to pass (Cremer and Cremer, 1978; Sheppard and Wilson, 1981; Brakenhoff et al., 1985). The emitted light is detected by a photomultiplier tube (PMT) or an avalanche photodiode (APD) and the image is then constructed by mapping the detected light in dependence of the position of the scanning spot. In principle, CLSM can achieve a better resolution than wide-field fluorescence microscopy but, to obtain a significant practical advantage, the pinhole needs to be closed to an extent where most of the light is discarded (Heintzmann et al., 2003). Alternatively, an interferometric detection technique could be used (Wicker et al., 2009).

## New strategies to improve optical resolution

Wide-field deconvolution and CLSM have long been the gold standards in optical bioimaging, but we are now witnessing a revolution in light microscopy that will fundamentally expand our perception of the cell. Recently, several new technologies, collectively termed super-resolution microscopy or nanoscopy, have been developed that break or bypass the classical diffraction limit and shift the optical resolution down to macromolecular or even molecular levels (Table I). Some of these technologies have now matured from the breadboard stage to commercially available imaging systems, making them increasingly attractive for broad applications and defining a new state of the art.

Conceptually, one can discern near-field from far-field methods and whether the subdiffraction resolution is based on a linear or nonlinear response of the sample to its locally illuminating (exciting or depleting) irradiance. The required nonlinearity is currently achieved by using reversible saturable optical fluorescence transitions (RESOLFT) between molecular states (Hofmann et al., 2005; Hell, 2007). Besides these saturable optical fluorescence transitions also other approaches, e.g., Rabi oscillations, could be used to generate the required nonlinear response.

Note that each of the novel imaging modes has its individual signal-to-noise consideration depending on various factors. A full discussion of this issue is beyond the scope of this review, but as a general rule, single-point scanning systems, albeit fundamentally limited in speed by fluorescence saturation effects, can have better signal-to-noise performance for thicker samples.

## Near-field methods

The most prominent near-field microscopy approach in cell biology utilizes the effect of total internal reflection at highly inclined angles at the glass–medium interface for the illumination of fluorophores (TIRF). The exponential decay of the evanescent field illumination intensity restricts excitation to a thin region extending to 100–200 nm behind the surface of the cover glass. Because there is effectively no signal from out-of-focus regions, the signal-to-noise ratio is improved in comparison to any computational method of out-of-focus blur removal. Notably, TIRF enhances only the axial resolution to below the diffraction limit. Although TIRF microscopy (TIRFM) has become a valuable and relatively easy-to-implement standard method in those fields of cell biology that deal with surface structures and dynamics (e.g., exo- and endocytosis in the plasma membrane, adhesion, and cytoskeleton), much of the cell interior is out of reach.

A sophisticated near-field approach, near-field scanning optical microscopy (SNOM, NSOM), works without objective lenses and instead scans samples with a very small physical aperture, e.g., positioned at the tip of a tapered glass fiber. In this case the evanescent wave is limited laterally as well as axially, thus bypassing the diffraction limit in all three dimensions of space, bringing the resolution to below 20 nm (Betzig and Trautman, 1992). However, the fundamental limitation remains

as only surface structures can be imaged (de Lange et al., 2001; Höppener et al., 2005; van Zanten et al., 2009).

## Far-field methods

Besides these rather specialized near-field approaches, three more generally applicable far-field methods, SIM, STED, and PALM/STORM, have been introduced. Their basic principles are outlined in Fig. 1 and discussed in detail below.

### Structured illumination microscopy (SIM).

Super-resolution structured illumination microscopy illuminates a sample with a series of sinusoidal striped patterns of high spatial frequency. This pattern is typically generated by laser light passing through a movable optical grating and projected via the objective onto the sample (Heintzmann and Cremer, 1999; Gustafsson, 2000). When illuminating a fluorescent sample containing fine structures, coarser interference patterns—moiré fringes—arise in the emission distribution and these coarse fringes can be transferred to the image plane by the microscope. By applying these bar code–like excitation patterns in different orientations and processing all acquired images using computer algorithms, a high-resolution image of the underlying structure can be generated (Fig. 1 A). These algorithms use the data (via various cross-correlation and minimization algorithms) to estimate the experimental parameters, such as the grating constant, phases and direction, unmix the multiple overlapping components in frequency space, and finally shift the moiré information back to the originating high frequency places to synthesize the image. With this approach the lateral resolution increases by a factor of two beyond the classical diffraction limit. With three-dimensional SIM (3D-SIM), an additional twofold increase in the axial resolution can be achieved by generating an excitation light modulation along the z-axis using three-beam interference (Gustafsson et al., 2008; Schermelleh et al., 2008) and processing a z-stack of images accordingly. Thus, with 3D-SIM an approximately eightfold smaller volume can be resolved in comparison to conventional microscopy (Fig. 2). To computationally reconstruct a three-dimensional dataset of a typical mammalian cell of 8- $\mu$ m height with a z-spacing of 125 nm, roughly 1,000 raw images (512  $\times$  512 pixels) are recorded. Because no special photophysics is needed, virtually all modern fluorescent labels can be used provided they are sufficiently photostable to accommodate the additional exposure cycles.

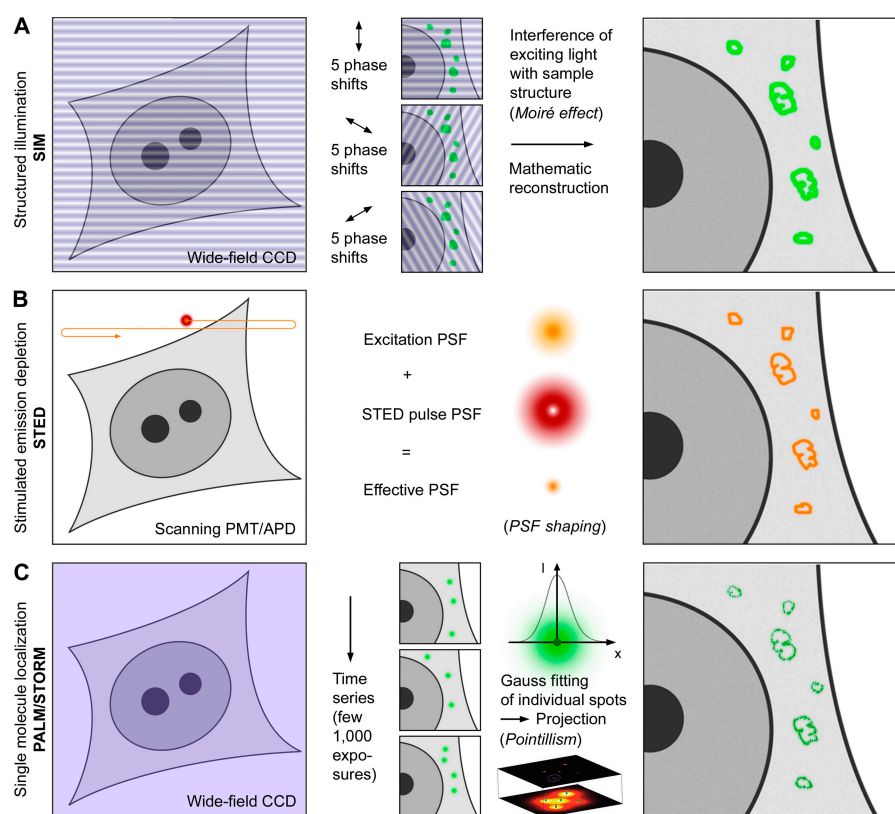
An attractive feature of structured illumination for cell biological applications is the fact that standard dyes and staining protocols can be used and multiple cellular structures can be simultaneously imaged with optical sectioning in three dimensions. Thus, fine patterns of replication foci could be resolved throughout the entire nucleus by 3D-SIM and quantitatively analyzed (Baddeley et al., 2010). The multicolor capability of 3D-SIM allows the imaging of several cellular components and the mapping of their relative positions in macromolecular complexes, enabling the study of their spatial relationship within the surrounding cellular contexts. One such example is the identification of interchromatin channels leading up to individual nuclear pores (Schermelleh et al., 2008). A multicolor 3D-SIM imaging of a mitotic cell is shown

Table 1. Super-resolution light microscopy methods

Principle	Near-field			Far-field			
	Small aperture scanning (no lens)	Evanescent wave illumination	Widefield + deconvolution	Confocal laser scanning	Moiré effect with structured illumination	PSF shaping with saturated emission depletion	Photoswitching and localization of single molecules (pointillism)
Acronym	SNOM/NSOM	TIRFM		CLSM	SIM (HELM, PEM) 3D-SIM	STED/CW-STED	PALM/FPALM/STORM/ dSTORM/PALMIRA
Illumination-emission dependence	Linear	Linear	Linear	Linear	Linear	Non-linear	Linear
Detector	Scanning PMT/APD	Widefield CCD/CMOS	Widefield CCD/CMOS	Scanning PMT/APD	Widefield CCD/CMOS	Scanning PMT/APD	Wide-field CCD/CMOS
XY-resolution	20–120 nm	200–300 nm	180–250 nm	180–250 nm	100–130 nm	20–100 nm	20–50 nm
Z-resolution	10 nm (nearfield range)	100 nm (nearfield range)	500–700 nm	500–700 nm	250–350 nm	560 nm (CW-STED) to 700 nm (100 nm with z-phase mask)	100 nm (TIRF) 20–30 nm (3D-STORM, TIRF) 75 nm (BP-FPALM, in plane)
Serial z-sectioning	No	No	Yes	Yes	Yes	Yes	Yes
Z stack range	N.A.	N.A.	100 µm	100 µm	10–20 µm	>20 µm	100 nm – few µm (BP-FPALM)
Dyes	Any	Any	Any	Any	Most conventional dyes (photostable)	Dyes require special characteristics (CW-STED works with many conventional dyes)	Dyes require special characteristics
Simultaneous colors	2	3	>3	>3	3	2	2
Temporal resolution for 512 x 512 image	s-min	ms	ms	ms-s	ms-s	ms-min	s-min
Energy load/intensity	Low	Low	Low	Medium	Medium	Medium-high	Medium-high
Live-cell imaging	Yes	Yes	Yes	Yes	Restricted (2D-TIRF)	Restricted	Restricted
Postprocessing required	No	No	Yes	No	Yes 9–25 raw images per slice	No	Yes >1,000 raw images per slice
Notes	No intracellular imaging	Restricted to region near the coverslip	Risk of artifacts; better for sparse samples	Reconstruction bears risk of artefacts	High excitation required; reconstruction bears risk of artefacts	Complex instrumentation; photobleaching	May require TIRF setup for best performance; labeling density is critical; performs better on particles and filaments as on volume stains
Dual lens implementation			iFM	4Pi	iFS	4 Pi-STED/iso-STED	iPALM
Z-resolution		70 nm		80 nm	100 nm	20–100 nm	10 nm (depth ~200 nm)

N.A., not applicable; N.D., not described.





**Figure 1. Super-resolution imaging principles.** (A) In SIM the sample plane is excited by a nonuniform wide-field illumination. Laser light passes through an optical grating, which generates a stripe-shaped sinusoidal interference pattern. This combines with the sample information originating from structures below the diffraction limit to generate moiré fringes. The image detected by the CCD camera thus contains high spatial frequency sample information shifted to a lower spatial frequency band that is transmitted through the objective. A mathematical reconstruction allows, from a series of 15 raw images per slice, to reconstruct a high-resolution image with doubled resolution in xy compared with wide-field resolution. In 3D-SIM additional doubling in the axial resolution is achieved by accounting for an additional modulation introduced along the axial direction. (B) In STED microscopy the focal plane is scanned with two overlapping laser beams, typically being pulsed with a mutual time delay. While the first laser excites the fluorophores, the second longer wavelength laser drives the fluorophores back to the ground state by the process of stimulated emission. A phase plate in the light path of the depletion laser generates a donut-shaped energy distribution, leaving only a small volume from which light can be emitted that is then being detected. Thus, the PSF is shaped to a volume smaller than the diffraction limit. (C) Single molecule localization microscopy assures that only a relatively low number of fluorophores are in the emitting (active) state. This is achieved

either by photoactivation, photoswitching, triplet state shelving, or blinking. These molecules are detected on the CCD camera as diffraction-limited spots, whose lateral position is determined with very high accuracy by a fit. Single molecule positions from several thousand raw images, each with a different subset of emitters, are then used to generate a density map featuring several hundred thousand single molecule positions within the plane of focus.

in Fig. 3 A. Recently, the first steps toward the imaging of living cells with SIM were taken to visualize mitochondria, tubulin, and kinesin dynamics in living cells (Hirvonen et al., 2009; Kner et al., 2009). However, the strict requirement of sample stability during the recording of the multiple images for each time-point makes a number of technical improvements and short cuts necessary. Most importantly, the acquisition of image sets has to be accelerated and at least initially confined to two dimensions by, e.g., TIRF.

It should be noted that the above-mentioned technique of structured illumination is related to an approach used for optical sectioning in wide-field microscopes (Wilson et al., 1998) that is commercialized under the names Apotome by Carl Zeiss, Inc., OptiGrid by Qioptiq, or the Angstrom system by Quorum/Leica. However, the illumination patterns used in these cases are too coarse to achieve a significant in-plane resolution improvement.

Structured illumination and strictly speaking even confocal microscopy make use of the resolution-enhancing influence of a spatially varying illumination. Spatial frequencies present in the excitation pattern can be added to Abbe's limit, which is valid for detection. In terms of the maximal spatial frequency, this yields a summation of the highest spatial frequency present in the illumination beam and the highest spatial frequency being detected. In other words, when the sample responds proportional to the illumination intensity, the Abbe limits for illumination and detection have to be added to form the new

resolution limit. Roughly twofold resolution enhancement can be achieved this way.

This addition starts with the assumption that the emitted (and thus also the detected) signal is proportional to the amount of illumination light hitting a fluorophore (or in other terms, the total PSF is effectively the product of excitation PSF and emission PSF). To circumvent the Abbe limit, one thus has to exploit properties of the illumination light interacting with the sample itself. Breaking the linear dependence between local illumination power and detection efficiency distribution enables microscopy modes that can go significantly beyond the limit imposed by Abbe's law on linear fluorescence microscopy.

This nonlinear response principle has been used in stimulated emission (Hell and Wichmann, 1994), ground state depletion (Hell and Kroug, 1995), and nonlinear saturated structured illumination microscopy (SSIM). SSIM is an extension of the above-described SIM concept using intense illumination saturating the fluorophore (Heintzmann et al., 2002; Heintzmann, 2003; Gustafsson, 2005). First experiments verified this concept, demonstrating a resolution better than 50 nm (Gustafsson, 2005). One limitation of direct saturation of fluorophores is that the required powers may lead to excessive bleaching, for example by absorption from the excited state or triplet state. More recent concepts (Hofmann et al., 2005; Hirvonen et al., 2009) have used photoswitchable fluorophores to achieve the required nonlinearity. To our knowledge, however,

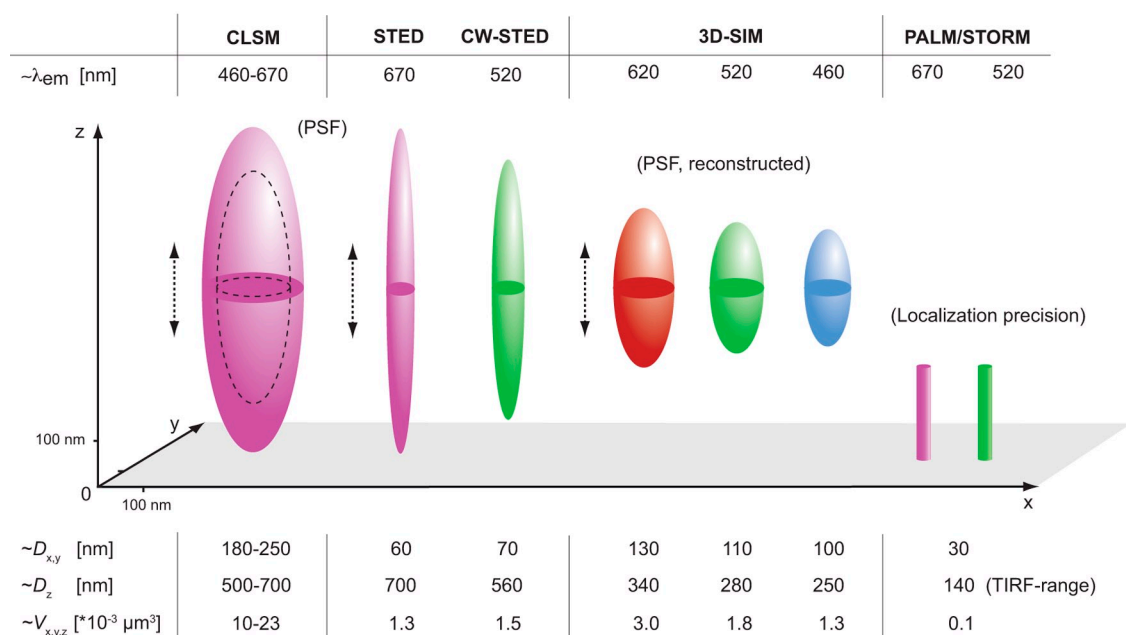


Figure 2. **Resolvable volumes obtained with current commercial super-resolution microscopes.** A schematic 3D representation of focal volumes is shown for the indicated emission maxima. The approximate lateral (x,y) and axial (z) resolution and resolvable volumes are listed. Note that STED/CW-STED and 3D-SIM can reach up to 20  $\mu m$  into the sample, whereas PALM/STORM is usually confined to the evanescent wave field near the sample bottom. It should be noted that deconvolution approaches can further improve STED resolution. For comparison the “focal volume” for PALM/STORM was estimated based on the localization precision in combination with the z-range of TIRF. These indications do not necessarily constitute actual resolution as many other effects (e.g., fluorophore orientation, local refractive index variations, flatfield quality of the camera, local aberrations, and statistical selection bias) influence image quality and final resolution.

demonstrations of high resolution in the 50-nm range have not yet been published.

**Stimulated emission depletion (STED).** A method using a nonlinear saturation process not for the excitation, but rather for a controlled de-excitation of previously excited fluorophores, is termed stimulated emission depletion (STED) microscopy (Fig. 1 B). Fluorophores slightly off the center of the excitation PSF will be illuminated with this stimulated emission depletion beam (which has a doughnut shape with a zero intensity at the very center generated by passage through an appropriate phase plate) and therefore de-excited back into the ground state of the fluorophore. Conveniently, this de-excitation also protects these fluorophores from photobleaching. In practice, attention needs to be paid to the correct timing, duration of the STED pulse, and a good quality of the zero intensity in the center STED beam. When this stimulated emission beam is driven into saturation, the excited state population gets depleted everywhere except for the very center, where the STED beam intensity is zero. Fluorescence from this central region is then spectrally separated from the further red-shifted STED beam and detected. The nonlinearity of the stimulated emission depletion is an essential feature to achieve high resolution images. Current experimental setups routinely achieve a resolution in the range of 30–80 nm.

The resolution of such a scanning microscope is essentially determined by the spot size of remaining excited fluorophores. The above principle of shaping the exciting point spread function with saturated emission depletion has been proposed and realized by Hell and colleagues (Hell and Wichmann, 1994; Klar et al., 2000; Dyba and Hell, 2002; Dyba et al., 2003).

STED microscopy has been successfully applied on biological samples (Kittel et al., 2006; Sieber et al., 2006; Willig et al., 2006), for example showing that synaptotagmin remains clustered after synaptic vesicle exocytosis (Willig et al., 2006). The commercially available TCS STED system from Leica reaches a lateral resolution down to 60 nm using picosecond pulses of a Ti/Sa laser for stimulated emission depletion (Fig. 2 and Fig. 3 B). The considerable costs of this technology have now been addressed in the TCS STED CW system that implements continuous wave lasers for excitation and depletion (Willig et al., 2007; Fölling et al., 2008a).

An important consideration is the choice of the right dye. The depletion laser wavelength should by no means fall into the excitation range of the dye, causing unwanted excitation in the region of fluorescence depletion. Also, the absorption of the red STED light by the excited singlet or triplet state of the fluorophore should be avoided to prevent severe photobleaching. Thus, the set of suitable dyes with appropriate photochemical properties (little Anti Stokes excitation, broad Stokes shift, high quantum yield) is limited compared with conventional methods. Less strict requirements are imposed by continuous-wave STED (CW-STED), which can be used with most conventional green-emitting dyes. Two-color STED (Donnert et al., 2007) has recently been demonstrated and is now commercially available, but further extension to three colors is currently hampered by the requirement of nonoverlapping excitation, emission, and depletion bands of wavelengths. Several recent publications have also demonstrated the application of STED in live-cell imaging experiments mostly investigating protein distribution and dynamics in membranes and vesicles (Hein et al., 2008, 2010;

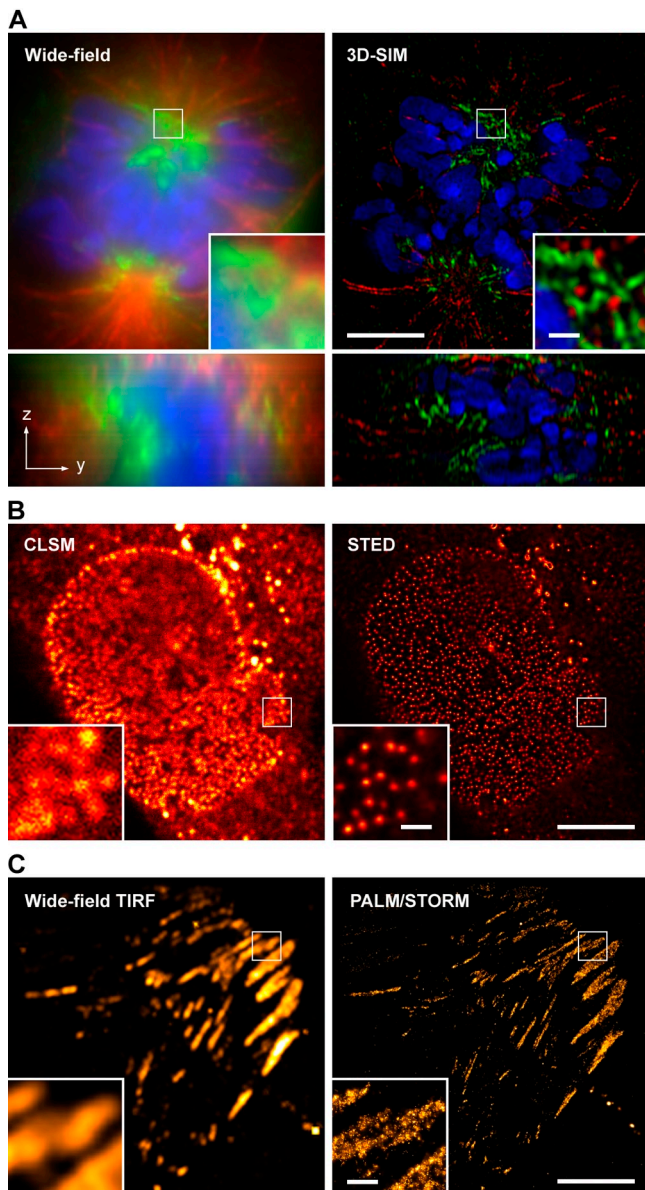


**Figure 3. Super-resolution microscopy of biological samples.** (A) Conventional wide-field image (left) and 3D-SIM image of a mouse C2C12 prometaphase cell stained with primary antibodies against lamin B and tubulin, and secondary antibodies conjugated to Alexa 488 (green) and Alexa 594 (red), respectively. Nuclear chromatin was stained with DAPI (blue). 3D image stacks were acquired with a DeltaVision OMX prototype system (Applied Precision). The bottom panel shows the respective orthogonal cross sections. (B) HeLa cell stained with primary antibodies against the nuclear pore complex protein Nup153 and secondary antibodies conjugated with ATTO647N. The image was acquired with a TCS STED confocal microscope (Leica). (C) TdEosFP-paxillin expressed in a Hep G2 cell to label adhesion complexes at the lower surface. The image was acquired on an ELYRA P.1 prototype system (Carl Zeiss, Inc.) using TIRF illumination. Single molecule positional information was projected from 10,000 frames recorded at 30 frames per second. On the left, signals were summed up to generate a TIRF image with conventional wide-field lateral resolution. Bars: 5  $\mu$ m (insets, 0.5  $\mu$ m).

Nägerl et al., 2008; Westphal et al., 2008; Eggeling et al., 2009; Opazo et al., 2010).

**Single molecule localization and composition (PALM/STORM).** A slightly more subtle nonlinear effect is based on the idea that many photons can be combined to

enhance the emission PSF. Under conditions where all photons are emitted from the same source, a simple fitting procedure on the image or the determination of the center of mass allows a more precise position determination than with the uncertainty of just a single emitted photon, which is stated by the width of the emission PSF. Although this principle has been known for a rather long time, most methods to separate such particles, which were based on their emission characteristics such as color (Bornfleth et al., 1998) or fluorescence lifetime (Heilemann et al., 2002), were limited to imaging only a few particles in close proximity. This changed drastically when it was realized that time could be used to separate the particles. The idea to assemble many such localized positions into high resolution images of the sample was termed pointillism, in analogy to the artistic painting technique (Lidke et al., 2005). The chance of detecting particles with overlapping signals in one image could be reduced to almost zero by limiting the number of simultaneously emitting particles (Betzig et al., 2006; Hess et al., 2006; Rust et al., 2006). This first became possible by using either photoactivatable dyes (e.g., paGFP), as in photoactivated localization microscopy (PALM) and fluorescence photoactivation localization microscopy (FPALM), or by using photoswitchable dye pairs (e.g., Cy3–Cy5) or photoswitchable proteins (e.g., EosFP), as in stochastic optical reconstruction microscopy (STORM). Such series of a few thousand images can then be processed into high resolution images typically reaching a resolution in the range of 30 nm (Fig. 1 C, Fig. 2, and Fig. 3 C).

It should be noted that the performance of these pointillistic methods critically depends on the labeling density and the imaged biological structure. Thus, they may perform better for imaging smaller or filamentous objects than dense and bulky structures. In view of the discussion of resolution limits above, it is now interesting to look at the predicted resolution of the pointillistic methods. Only considering the statistical noise of photon counting and assuming the point spread functions to be of Gaussian shape, the laws of Gaussian error propagation state that the precision of localization scales with the inverse square root  $N^{-1/2}$  of the number of detected photons. In other words, the resolution is limited by photon statistics or the more photons are collected the better is the resolution.

Variations of this method have been published by numerous groups adding new acronyms, such as SPDM (spectral precision distance measurement; Bornfleth et al., 1998; Lemmer et al., 2009), PALMIRA (PALM with independently running acquisition; Egner et al., 2007), GSDIM (ground state depletion and individual molecule return; Fölling et al., 2008b), or dSTORM (direct STORM; Heilemann et al., 2008). The latter use the reversible photoswitching of organic fluorochromes to a long-lived dark state (e.g., the triplet state or charge transfer complexes), which extends this method in principle to conventional dyes.

Two-color applications on biological samples have been demonstrated for most approaches (Bates et al., 2007; Bock et al., 2007; Shroff et al., 2007; Bossi et al., 2008; Gunkel et al., 2009; Subach et al., 2009; van de Linde et al., 2009) and has been successfully used to map vertebrate kinetochore components



on stretched chromatin fibers (Ribeiro et al., 2010). Recent implementations have also demonstrated the ability to localize single molecules with subdiffraction accuracy (50–80 nm) in the axial direction over an extended imaging depth of a few microns by either introducing an astigmatism, as in 3D STORM (Huang et al., 2008a,b), by a double-plane detection in biplane (BP) FPALM (Jüette et al., 2008), or by engineering a double helix-shaped point spread function (DH-PSF; Pavani et al., 2009). The utility of these techniques for live-cell imaging has been demonstrated (Hess et al., 2007), although it is still restricted to small cellular subregions or rather slow processes in 2D. It will still take time and further engineering until these technical developments find their way into commercial systems. Nonetheless, the number of recent publications indicates that the field is rapidly progressing toward 3D live-cell studies.

### Opposing objective approaches

Conventional and super-resolution techniques can be combined with interferometric configurations to further enhance the axial resolution. In 4Pi microscopy, the concept of confocal microscopy is extended by having two precisely aligned identical objective lenses act as a single lens (Sheppard and Matthews, 1987; Hell et al., 1994a,b; Schrader et al., 1997, 1998; Egner et al., 2002, 2004) to achieve a z-resolution down to 80 nm. 4Pi microscopy has been successfully applied to study the details of the nuclear pore complex (Hüve et al., 2008) and to investigate H2AX at sites of DNA damage (Bewersdorf et al., 2006). Similarly, double-sided illumination and/or detection can enhance the axial performance of wide-field microscopy as in I<sup>2</sup>M (Gustafsson et al., 1999) or SMI (Albrecht et al., 2002), structured illumination as in I<sup>2</sup>S (Shao et al., 2008), STED as in isoSTED (Schmidt et al., 2008, 2009), and PALM as in iPALM (Shtengel et al., 2009). All these techniques require extremely precise alignment of the two opposing light paths via piezo-electric control and extensive preparatory alignment procedures. In addition, the sample preparation and embedding requires extra care. Coherent opposing lens arrangements are also very sensitive to temperature shifts and are altogether technically very demanding.

### Present trade-offs

As diverse as these new technologies are, so are their opportunities and trade-offs for applications in cell biology. Therefore, when choosing the best technology for a given cell biological question, one has to match experimental requirements with technical performance. For comparison, the technical performance data of several present super-resolution methods were compiled from recent publications (Table I). Some commercially available technologies improve lateral but not axial resolution, which makes them ideal for studies of flat structures such as membranes but less suited for extended 3D structures like the nucleus. Similarly, the possibility to image three or four cellular components in 3D with conventional staining protocols might outweigh the higher lateral resolution available from an alternative method (Fig. 2). Optimum resolution should be weighed against versatility, suitability for live-cell applications, and the simultaneous detection of multiple components.

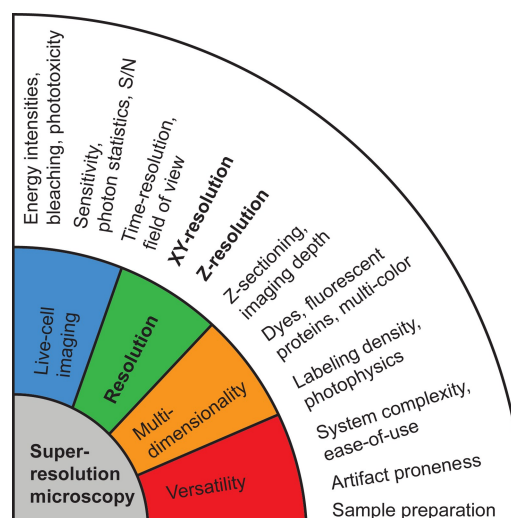


**Figure 4. Challenges and trade-offs in super-resolution fluorescence microscopy.** Although the nominal lateral (xy) and axial (z) resolution of a microscope is the most prominent system parameter, the usefulness for broader or routine application depends on a wealth of additional criteria. This includes the ability to image time series of living samples and multi-dimensional imaging (3D sectioning with multiple wavelength), as well as soft criteria, such as the easy applicability and the reliability of the results. Notably, none of the currently available super-resolution technologies fulfill all criteria.

For example, in developmental biology the ability to image entire embryos in three dimensions over long time periods may be more important than absolute resolution. Of particular interest for biological applications is light sheet-based microscopy, as large specimens can be imaged with a substantially enhanced axial resolution down to 0.4  $\mu\text{m}$  and minimal phototoxicity (Verveer et al., 2007). Thus, the embryogenesis of flies and zebrafish was successfully imaged with an isotropic resolution using selective plane illumination microscopy (SPIM) and an orthogonal camera-based detection (Huisken et al., 2004; Keller et al., 2008). Also, one has to keep in mind that some of the published performance benchmarks are “world records” established by experts and may not be easily obtained in a routine laboratory. Multi-user environments should consider the manageability and the availability of the necessary technical expertise to run and maintain a given system. Thus, the complexity and user-friendliness of the system, the susceptibility to artifacts, and the demands for special sample preparation should be taken into account (Fig. 4).

Most challenging still is the full-fledged implementation of super-resolution in live-cell microscopy, i.e., the monitoring of dynamic processes with multi-dimensional time-series at super-resolution without affecting the physiology or viability of the cell. In case of samples with a constant density of fluorophores, higher resolution for the same field of view automatically means less fluorophores per volume element (voxel) as the interrogated volume becomes smaller, e.g., a twofold better resolution in 3D entails an eightfold smaller volume, meaning also eightfold less fluorophores at the same labeling density. To compensate the drop in brightness and achieve a similar signal to noise as in the normal resolution image, the excitation intensity could be increased which would, however, also increase



phototoxicity and adversely affect living cells. Alternatively, the imaging time could be prolonged, which makes it more likely that the cells or subcellular components move within this extended image acquisition time. This is especially true as some super-resolution methods are already slower to begin with. However, it has to be noted that the situation becomes more relaxed when the structure of interest is essentially one-dimensional (filaments) or even point-like (vesicles). In the latter case, all of the signal would only be present in the few voxels covering the vesicle, allowing the image quality to be retained even at an identical number of totally present fluorophores (or detected photons). First attempts toward live imaging succeeded by carefully matching the appropriate technologies to the imaging problem at hand and by being willing to accept compromises in versatility and scope (Hess et al., 2007; Kner et al., 2009; Nägerl et al., 2008; Shroff et al., 2008; Westphal et al., 2008).

### Future perspectives/outlook

Just a few years after their first implementation, these rapidly developing super-resolution techniques have already had a clear impact on modern cell biology. Although all these techniques represent a formidable advance over conventional microscopy, they also have their specific strengths and weaknesses as discussed above. At present, there is no ideal system available that could combine the highest spatial resolution laterally and axially along with multicolor capabilities and temporal resolution for live-cell applications. Although there are inherent limitations, such as photon statistics that create a trade-off between spatial and temporal resolution, there is still room for improvement. The development of more sensitive detectors/cameras and flexible lasers together with fast-switching optical elements, such as acousto-optical deflectors or liquid crystal spatial light modulators, will further speed up image acquisition and increase the temporal resolution. Increased sensitivity will enable lower excitation intensities and thereby reduce the phototoxic effects on the physiology and viability of the observed cells. The implementation of interferometric and nonlinear approaches in commercial products is still technically challenging but will likely be an important step toward new performance benchmarks. Another promising direction is the combination of super-resolution light microscopy with EM techniques like the correlative PALM-TEM (Betzig et al., 2006). Such combined approaches provide valuable contextual information for the study of cellular nanostructures. The development of new switchable and/or photostable fluorophores (Fölling et al., 2007; Fernández-Suárez and Ting, 2008; Schröder et al., 2009; Subach et al., 2009) and the chemical modulation of photophysical properties (Donnert et al., 2006; Staudt et al., 2007; Steinhauer et al., 2008; Vogelsang et al., 2008; Bogdanov et al., 2009) will mark further improvements. Finally, new types of molecular probes such as extremely small and stable chromobodies that can detect antigens in living cells (Rothbauer et al., 2006) in combination with these super-resolution techniques will further expand the repertoire of modern cell biology.

A formidable challenge remains the imaging of the thick biological specimen, as the sample itself is part of the optical system. The natural optical anisotropy of these samples foils all

engineering attempts to build perfect systems. Future solutions may not eliminate this problem but could map the optical anisotropy of cells and then compensate for it by post processing and/or adaptive optics (Kam et al., 2001; Booth et al., 2002; Ji et al., 2010), similar to what is already practiced in astronomy. In this emerging field a number of further innovations are currently being developed. Significant engineering challenges remain before these next-generation super-resolution technologies become widely available. As the first super-resolution microscopes are now becoming commercially available, many new and exciting insights into cellular structure and function are to be expected in the near future.

We thank representatives of Leica, Carl Zeiss, Inc., and Applied Precision for technical support and enlightening discussions.

Research in the authors' laboratories is supported by grants from the Deutsche Forschungsgemeinschaft (SFB TR5), the Bioimaging Network, the Nano-systems Initiative Munich, the Center for Nanoscience (to L. Schermelleh and H. Leonhardt), and the Engineering and Physical Sciences Research Council (to R. Heintzmann).

Submitted: 2 February 2010

Accepted: 22 June 2010

## References

- Abbe, E. 1873. Beiträge zur Theorie des Mikroskops und der mikroskopischen Wahrnehmung. *Archiv für mikroskopische Anatomie*. 9:413–418.
- Agard, D.A., and J.W. Sedat. 1983. Three-dimensional architecture of a polytene nucleus. *Nature*. 302:676–681. doi:10.1038/302676a0
- Agard, D.A., Y. Hiraoka, P. Shaw, and J.W. Sedat. 1989. Fluorescence microscopy in three dimensions. *Methods Cell Biol.* 30:353–377. doi:10.1016/S0091-679X(08)60986-3
- Albrecht, B., A.V. Failla, A. Schweitzer, and C. Cremer. 2002. Spatially modulated illumination microscopy allows axial distance resolution in the nanometer range. *Appl. Opt.* 41:80–87. doi:10.1364/AO.41.000080
- Baddeley, D., V.O. Chagin, L. Schermelleh, S. Martin, A. Pombo, P.M. Carlton, A. Gahl, P. Domaing, U. Birk, H. Leonhardt, et al. 2010. Measurement of replication structures at the nanometer scale using super-resolution light microscopy. *Nucleic Acids Res.* 38:e8. doi:10.1093/nar/gkp901
- Bates, M., B. Huang, G.T. Dempsey, and X. Zhuang. 2007. Multicolor super-resolution imaging with photo-switchable fluorescent probes. *Science*. 317:1749–1753. doi:10.1126/science.1146598
- Betzig, E., and J.K. Trautman. 1992. Near-field optics: microscopy, spectroscopy, and surface modification beyond the diffraction limit. *Science*. 257:189–195. doi:10.1126/science.257.5067.189
- Betzig, E., G.H. Patterson, R. Sougrat, O.W. Lindwasser, S. Olenych, J.S. Bonifacino, M.W. Davidson, J. Lippincott-Schwartz, and H.F. Hess. 2006. Imaging intracellular fluorescent proteins at nanometer resolution. *Science*. 313:1642–1645. doi:10.1126/science.1127344
- Bewersdorf, J., R. Schmidt, and S.W. Hell. 2006. Comparison of I5M and 4Pi-microscopy. *J. Microsc.* 222:105–117. doi:10.1111/j.1365-2818.2006.01578.x
- Bock, H., C. Geisler, C.A. Wurm, C. von Middendorff, S. Jakobs, A. Schönle, A. Egner, S.W. Hell, and C. Eggeling. 2007. Two-color far-field fluorescence nanoscopy based on photoswitching emitters. *Appl. Phys. B*. 88:161–165. doi:10.1007/s00340-007-2729-0
- Bogdanov, A.M., E.A. Bogdanova, D.M. Chudakov, T.V. Gorodnicheva, S. Lukyanov, and K.A. Lukyanov. 2009. Cell culture medium affects GFP photostability: a solution. *Nat. Methods*. 6:859–860. doi:10.1038/nmeth1209-859
- Booth, M.J., M.A. Neil, R. Juskaitis, and T. Wilson. 2002. Adaptive aberration correction in a confocal microscope. *Proc. Natl. Acad. Sci. USA*. 99:5788–5792. doi:10.1073/pnas.082544799
- Bornfleth, H., K. Sätzler, R. Eils, and C. Cremer. 1998. High-precision distance measurements and volume-conserving segmentation of objects near and below the resolution limit in three-dimensional confocal fluorescence microscopy. *J. Microsc.* 189:118–136. doi:10.1046/j.1365-2818.1998.00276.x
- Bossi, M., J. Fölling, V.N. Belov, V.P. Boyarskiy, R. Medda, A. Egner, C. Eggeling, A. Schönle, and S.W. Hell. 2008. Multicolor far-field fluorescence nanoscopy through isolated detection of distinct molecular species. *Nano Lett.* 8:2463–2468. doi:10.1021/nl801471d

- Brakenhoff, G.J., H.T. van der Voort, E.A. van Spronsen, W.A. Linnemans, and N. Nanninga. 1985. Three-dimensional chromatin distribution in neuroblastoma nuclei shown by confocal scanning laser microscopy. *Nature*. 317:748–749. doi:10.1038/317748a0
- Conchello, J.A., and J.W. Lichtman. 2005. Optical sectioning microscopy. *Nat. Methods*. 2:920–931. doi:10.1038/nmeth815
- Cremer, C., and T. Cremer. 1978. Considerations on a laser-scanning-microscope with high resolution and depth of field. *Microsc. Acta*. 81:31–44.
- de Lange, F., A. Cambi, R. Huijbens, B. de Bakker, W. Rensen, M. Garcia-Parajo, N. van Hulst, and C.G. Figdor. 2001. Cell biology beyond the diffraction limit: near-field scanning optical microscopy. *J. Cell Sci.* 114:4153–4160.
- Donnert, G., J. Keller, R. Medda, M.A. Andrei, S.O. Rizzoli, R. Lührmann, R. Jahn, C. Eggeling, and S.W. Hell. 2006. Macromolecular-scale resolution in biological fluorescence microscopy. *Proc. Natl. Acad. Sci. USA*. 103:11440–11445. doi:10.1073/pnas.0604965103
- Donnert, G., J. Keller, C.A. Wurm, S.O. Rizzoli, V. Westphal, A. Schönlé, R. Jahn, S. Jakobs, C. Eggeling, and S.W. Hell. 2007. Two-color far-field fluorescence nanoscopy. *Biophys. J.* 92:L67–L69. doi:10.1529/biophysj.107.104497
- Dyba, M., and S.W. Hell. 2002. Focal spots of size  $\lambda/23$  open up far-field fluorescence microscopy at 33 nm axial resolution. *Phys. Rev. Lett.* 88:163901. doi:10.1103/PhysRevLett.88.163901
- Dyba, M., S. Jakobs, and S.W. Hell. 2003. Immunofluorescence stimulated emission depletion microscopy. *Nat. Biotechnol.* 21:1303–1304. doi:10.1038/nbt897
- Eggeling, C., C. Ringemann, R. Medda, G. Schwarzmann, K. Sandhoff, S. Polyakova, V.N. Belov, B. Hein, C. von Middendorff, A. Schönlé, and S.W. Hell. 2009. Direct observation of the nanoscale dynamics of membrane lipids in a living cell. *Nature*. 457:1159–1162. doi:10.1038/nature07596
- Egner, A., S. Jakobs, and S.W. Hell. 2002. Fast 100-nm resolution three-dimensional microscope reveals structural plasticity of mitochondria in live yeast. *Proc. Natl. Acad. Sci. USA*. 99:3370–3375. doi:10.1073/pnas.052545099
- Egner, A., S. Verrier, A. Goroshkov, H.D. Söling, and S.W. Hell. 2004. 4Pi-microscopy of the Golgi apparatus in live mammalian cells. *J. Struct. Biol.* 147:70–76. doi:10.1016/j.jsb.2003.10.006
- Egner, A., C. Geisler, C. von Middendorff, H. Bock, D. Wenzel, R. Medda, M. Andresen, A.C. Stiel, S. Jakobs, C. Eggeling, et al. 2007. Fluorescence nanoscopy in whole cells by asynchronous localization of photoswitching emitters. *Biophys. J.* 93:3285–3290. doi:10.1529/biophysj.107.112201
- Fernández-Suárez, M., and A.Y. Ting. 2008. Fluorescent probes for super-resolution imaging in living cells. *Nat. Rev. Mol. Cell Biol.* 9:929–943. doi:10.1038/nrm2531
- Fölling, J., V. Belov, R. Kunetsky, R. Medda, A. Schönlé, A. Egner, C. Eggeling, M. Bossi, and S.W. Hell. 2007. Photochromic rhodamines provide nanoscopy with optical sectioning. *Angew. Chem. Int. Ed. Engl.* 46:6266–6270. doi:10.1002/anie.200702167
- Fölling, J., V. Belov, D. Riedel, A. Schönlé, A. Egner, C. Eggeling, M. Bossi, and S.W. Hell. 2008a. Fluorescence nanoscopy with optical sectioning by two-photon induced molecular switching using continuous-wave lasers. *ChemPhysChem*. 9:321–326. doi:10.1002/cphc.200700655
- Fölling, J., M. Bossi, H. Bock, R. Medda, C.A. Wurm, B. Hein, S. Jakobs, C. Eggeling, and S.W. Hell. 2008b. Fluorescence nanoscopy by ground-state depletion and single-molecule return. *Nat. Methods*. 5:943–945. doi:10.1038/nmeth.1257
- Giepmans, B.N., S.R. Adams, M.H. Ellisman, and R.Y. Tsien. 2006. The fluorescent toolbox for assessing protein location and function. *Science*. 312:217–224. doi:10.1126/science.1124618
- Gunkel, M., F. Erdel, K. Rippe, P. Lemmer, R. Kaufmann, C. Hörmann, R. Amberger, and C. Cremer. 2009. Dual color localization microscopy of cellular nanostructures. *Biotechnol. J.* 4:927–938. doi:10.1002/biot.200900005
- Gustafsson, M.G. 2000. Surpassing the lateral resolution limit by a factor of two using structured illumination microscopy. *J. Microsc.* 198:82–87. doi:10.1046/j.1365-2818.2000.00710.x
- Gustafsson, M.G. 2005. Nonlinear structured-illumination microscopy: wide-field fluorescence imaging with theoretically unlimited resolution. *Proc. Natl. Acad. Sci. USA*. 102:13081–13086. doi:10.1073/pnas.0406877102
- Gustafsson, M.G., D.A. Agard, and J.W. Sedat. 1999. I5M: 3D widefield light microscopy with better than 100 nm axial resolution. *J. Microsc.* 195:10–16. doi:10.1046/j.1365-2818.1999.00576.x
- Gustafsson, M.G., L. Shao, P.M. Carlton, C.J. Wang, I.N. Golubovskaya, W.Z. Cande, D.A. Agard, and J.W. Sedat. 2008. Three-dimensional resolution doubling in wide-field fluorescence microscopy by structured illumination. *Biophys. J.* 94:4957–4970. doi:10.1529/biophysj.107.120345
- Heilemann, M., D.P. Herten, R. Heintzmann, C. Cremer, C. Müller, P. Tinnefeld, K.D. Weston, J. Wolfrum, and M. Sauer. 2002. High-resolution colocalization of single dye molecules by fluorescence lifetime imaging microscopy. *Anal. Chem.* 74:3511–3517. doi:10.1021/ac025576g
- Heilemann, M., S. van de Linde, M. Schüttelpelz, R. Kasper, B. Seefeldt, A. Mukherjee, P. Tinnefeld, and M. Sauer. 2008. Subdiffraction-resolution fluorescence imaging with conventional fluorescent probes. *Angew. Chem. Int. Ed. Engl.* 47:6172–6176. doi:10.1002/anie.200802376
- Hein, B., K.I. Willig, and S.W. Hell. 2008. Stimulated emission depletion (STED) nanoscopy of a fluorescent protein-labeled organelle inside a living cell. *Proc. Natl. Acad. Sci. USA*. 105:14271–14276. doi:10.1073/pnas.0807705105
- Hein, B., K.I. Willig, C.A. Wurm, V. Westphal, S. Jakobs, and S.W. Hell. 2010. Stimulated emission depletion nanoscopy of living cells using SNAP-tag fusion proteins. *Biophys. J.* 98:158–163. doi:10.1016/j.bpj.2009.09.053
- Heintzmann, R. 2003. Saturated patterned excitation microscopy with two-dimensional excitation patterns. *Micron*. 34:283–291. doi:10.1016/S0968-4328(03)00053-2
- Heintzmann, R. 2007. Estimating missing information by maximum likelihood deconvolution. *Micron*. 38:136–144. doi:10.1016/j.micron.2006.07.009
- Heintzmann, R., and C. Cremer. 1999. Lateral modulated excitation microscopy: Improvement of resolution by using a diffraction grating. *Proc. SPIE*. 3568:185–195. doi:10.1117/12.336833
- Heintzmann, R., T.M. Jovin, and C. Cremer. 2002. Saturated patterned excitation microscopy—a concept for optical resolution improvement. *J. Opt. Soc. Am. A Opt. Image Sci. Vis.* 19:1599–1609. doi:10.1364/JOSAA.19.001599
- Heintzmann, R., V. Sarafis, P. Munroe, J. Nailon, Q.S. Hanley, and T.M. Jovin. 2003. Resolution enhancement by subtraction of confocal signals taken at different pinhole sizes. *Micron*. 34:293–300. doi:10.1016/S0968-4328(03)00054-4
- Hell, S.W. 2007. Far-field optical nanoscopy. *Science*. 316:1153–1158. doi:10.1126/science.1137395
- Hell, S.W., and M. Kroug. 1995. Ground-state depletion fluorescence microscopy, a concept for breaking the diffraction resolution limit. *Appl. Phys. B*. 60:495–497. doi:10.1007/BF01081333
- Hell, S.W., and J. Wichmann. 1994. Breaking the diffraction resolution limit by stimulated emission: stimulated-emission-depletion fluorescence microscopy. *Opt. Lett.* 19:780–782. doi:10.1364/OL.19.000780
- Hell, S.W., S. Lindek, C. Cremer, and E.H. Stelzer. 1994a. Measurement of the 4pi-confocal point spread function proves 75 nm axial resolution. *Appl. Phys. Lett.* 64:1335–1337. doi:10.1063/1.111926
- Hell, S.W., E.H. Stelzer, S. Lindek, and C. Cremer. 1994b. Confocal microscopy with an increased detection aperture: type-B 4Pi confocal microscopy. *Opt. Lett.* 19:222. doi:10.1364/OL.19.000222
- Hess, S.T., T.P. Girirajan, and M.D. Mason. 2006. Ultra-high resolution imaging by fluorescence photoactivation localization microscopy. *Biophys. J.* 91:4258–4272. doi:10.1529/biophysj.106.091116
- Hess, S.T., T.J. Gould, M.V. Gudheti, S.A. Maas, K.D. Mills, and J. Zimmerberg. 2007. Dynamic clustered distribution of hemagglutinin resolved at 40 nm in living cell membranes discriminates between raft theories. *Proc. Natl. Acad. Sci. USA*. 104:17370–17375. doi:10.1073/pnas.0708066104
- Hirvonen, L.M., K. Wicker, O. Mandula, and R. Heintzmann. 2009. Structured illumination microscopy of a living cell. *Eur. Biophys. J.* 38:807–812. doi:10.1007/s00249-009-0501-6
- Hofmann, M., C. Eggeling, S. Jakobs, and S.W. Hell. 2005. Breaking the diffraction barrier in fluorescence microscopy at low light intensities by using reversibly photoswitchable proteins. *Proc. Natl. Acad. Sci. USA*. 102:17565–17569. doi:10.1073/pnas.0506010102
- Höppener, C., J.P. Siebrasse, R. Peters, U. Kubitschek, and A. Naber. 2005. High-resolution near-field optical imaging of single nuclear pore complexes under physiological conditions. *Biophys. J.* 88:3681–3688. doi:10.1529/biophysj.104.051458
- Huang, B., S.A. Jones, B. Brandenburg, and X. Zhuang. 2008a. Whole-cell 3D STORM reveals interactions between cellular structures with nanometer-scale resolution. *Nat. Methods*. 5:1047–1052. doi:10.1038/nmeth.1274
- Huang, B., W. Wang, M. Bates, and X. Zhuang. 2008b. Three-dimensional super-resolution imaging by stochastic optical reconstruction microscopy. *Science*. 319:810–813. doi:10.1126/science.1153529
- Huiskens, J., J. Swoger, F. Del Bene, J. Wittbrodt, and E.H. Stelzer. 2004. Optical sectioning deep inside live embryos by selective plane illumination microscopy. *Science*. 305:1007–1009. doi:10.1126/science.1100035
- Hüve, J., R. Wesselmann, M. Kahms, and R. Peters. 2008. 4Pi microscopy of the nuclear pore complex. *Biophys. J.* 95:877–885. doi:10.1529/biophysj.107.127449
- Ji, N., D.E. Milkie, and E. Betzig. 2010. Adaptive optics via pupil segmentation for high-resolution imaging in biological tissues. *Nat. Methods*. 7:141–147. doi:10.1038/nmeth.1411
- Juette, M.F., T.J. Gould, M.D. Lessard, M.J. Mlodzikowski, B.S. Nagpure, B.T. Bennett, S.T. Hess, and J. Bewersdorff. 2008. Three-dimensional sub-100

- nm resolution fluorescence microscopy of thick samples. *Nat. Methods*. 5:527–529. doi:10.1038/nmeth.1211
- Kam, Z., B. Hanser, M.G. Gustafsson, D.A. Agard, and J.W. Sedat. 2001. Computational adaptive optics for live three-dimensional biological imaging. *Proc. Natl. Acad. Sci. USA*. 98:3790–3795. doi:10.1073/pnas.071275698
- Keller, P.J., A.D. Schmidt, J. Wittbrodt, and E.H. Stelzer. 2008. Reconstruction of zebrafish early embryonic development by scanned light sheet microscopy. *Science*. 322:1065–1069. doi:10.1126/science.1162493
- Kittel, R.J., C. Wichmann, T.M. Rasse, W. Fouquet, M. Schmidt, A. Schmid, D.A. Wagh, C. Pawlu, R.R. Kellner, K.I. Willig, et al. 2006. Bruchpilot promotes active zone assembly, Ca<sup>2+</sup> channel clustering, and vesicle release. *Science*. 312:1051–1054. doi:10.1126/science.1126308
- Klar, T.A., S. Jakobs, M. Dyba, A. Egner, and S.W. Hell. 2000. Fluorescence microscopy with diffraction resolution barrier broken by stimulated emission. *Proc. Natl. Acad. Sci. USA*. 97:8206–8210. doi:10.1073/pnas.97.15.8206
- Kner, P., B.B. Chhun, E.R. Griffis, L. Winoto, and M.G. Gustafsson. 2009. Super-resolution video microscopy of live cells by structured illumination. *Nat. Methods*. 6:339–342. doi:10.1038/nmeth.1324
- Lemmer, P., M. Gunkel, Y. Weiland, P. Müller, D. Baddeley, R. Kaufmann, A. Urlich, H. Eipel, R. Amberger, M. Hausmann, and C. Cremer. 2009. Using conventional fluorescent markers for far-field fluorescence localization nanoscopy allows resolution in the 10-nm range. *J. Microsc.* 235:163–171. doi:10.1111/j.1365-2818.2009.03196.x
- Lidke, K., B. Rieger, T. Jovin, and R. Heintzmann. 2005. Superresolution by localization of quantum dots using blinking statistics. *Opt. Express*. 13:7052–7062. doi:10.1364/OPEX.13.007052
- Nägerl, U.V., K.I. Willig, B. Hein, S.W. Hell, and T. Bonhoeffer. 2008. Live-cell imaging of dendritic spines by STED microscopy. *Proc. Natl. Acad. Sci. USA*. 105:18982–18987. doi:10.1073/pnas.0810028105
- Opazo, F., A. Punge, J. Bückers, P. Hoopmann, L. Kastrop, S.W. Hell, and S.O. Rizzoli. 2010. Limited intermixing of synaptic vesicle components upon vesicle recycling. *Traffic*. 11:800–812. doi:10.1111/j.1600-0854.2010.01058.x
- Pavani, S.R., M.A. Thompson, J.S. Biteen, S.J. Lord, N. Liu, R.J. Twieg, R. Piestun, and W.E. Moerner. 2009. Three-dimensional, single-molecule fluorescence imaging beyond the diffraction limit by using a double-helix point spread function. *Proc. Natl. Acad. Sci. USA*. 106:2995–2999. doi:10.1073/pnas.0900245106
- Rayleigh, L. 1896. On the theory of optical images, with special reference to the microscope. *Philos. Mag.* 42:167–195.
- Ribeiro, S.A., P. Vagnarelli, Y. Dong, T. Hori, B.F. McEwen, T. Fukagawa, C. Flors, and W.C. Earnshaw. 2010. A super-resolution map of the vertebrate kinetochore. *Proc. Natl. Acad. Sci. USA*. 107:10484–10489. doi:10.1073/pnas.1002325107
- Rothbauer, U., K. Zolghadr, S. Tillib, D. Nowak, L. Schermelleh, A. Gahl, N. Backmann, K. Conrath, S. Muyltermans, M.C. Cardoso, and H. Leonhardt. 2006. Targeting and tracing antigens in live cells with fluorescent nanobodies. *Nat. Methods*. 3:887–889. doi:10.1038/nmeth953
- Rust, M.J., M. Bates, and X. Zhuang. 2006. Sub-diffraction-limit imaging by stochastic optical reconstruction microscopy (STORM). *Nat. Methods*. 3:793–795. doi:10.1038/nmeth929
- Schermelleh, L., P.M. Carlton, S. Haase, L. Shao, L. Winoto, P. Kner, B. Burke, M.C. Cardoso, D.A. Agard, M.G. Gustafsson, et al. 2008. Subdiffraction multicolor imaging of the nuclear periphery with 3D structured illumination microscopy. *Science*. 320:1332–1336. doi:10.1126/science.1156947
- Schmidt, R., C.A. Wurm, S. Jakobs, J. Engelhardt, A. Egner, and S.W. Hell. 2008. Spherical nanosized focal spot unravels the interior of cells. *Nat. Methods*. 5:539–544. doi:10.1038/nmeth.1214
- Schmidt, R., C.A. Wurm, A. Punge, A. Egner, S. Jakobs, and S.W. Hell. 2009. Mitochondrial cristae revealed with focused light. *Nano Lett.* 9:2508–2510. doi:10.1021/nl901398t
- Schrader, M., M. Kozubek, S.W. Hell, and T. Wilson. 1997. Optical transfer functions of 4Pi confocal microscopes: theory and experiment. *Opt. Lett.* 22:436–438. doi:10.1364/OL.22.000436
- Schrader, M., K. Bahlmann, G. Giese, and S.W. Hell. 1998. 4Pi-confocal imaging in fixed biological specimens. *Biophys. J.* 75:1659–1668. doi:10.1016/S0006-3495(98)77608-8
- Schröder, J., H. Benink, M. Dyba, and G.V. Los. 2009. In vivo labeling method using a genetic construct for nanoscale resolution microscopy. *Biophys. J.* 96:L01–L03.
- Shao, L., B. Isaac, S. Uzawa, D.A. Agard, J.W. Sedat, and M.G. Gustafsson. 2008. ISS: wide-field light microscopy with 100-nm-scale resolution in three dimensions. *Biophys. J.* 94:4971–4983. doi:10.1529/biophysj.107.120352
- Sheppard, C.J., and T. Wilson. 1981. The theory of the direct-view confocal microscope. *J. Microsc.* 124:107–117.
- Sheppard, G.J.R., and H.J. Matthews. 1987. Imaging in high-aperture optical systems. *J. Opt. Soc. Am. A*. 4:1354–1360. doi:10.1364/JOSAA.4.001354
- Shroff, H., C.G. Galbraith, J.A. Galbraith, H. White, J. Gillette, S. Olenych, M.W. Davidson, and E. Betzig. 2007. Dual-color superresolution imaging of genetically expressed probes within individual adhesion complexes. *Proc. Natl. Acad. Sci. USA*. 104:20308–20313. doi:10.1073/pnas.0710517105
- Shroff, H., C.G. Galbraith, J.A. Galbraith, and E. Betzig. 2008. Live-cell photo-activated localization microscopy of nanoscale adhesion dynamics. *Nat. Methods*. 5:417–423. doi:10.1038/nmeth.1202
- Shtengel, G., J.A. Galbraith, C.G. Galbraith, J. Lippincott-Schwartz, J.M. Gillette, S. Manley, R. Sougrat, C.M. Waterman, P. Kanchanawong, M.W. Davidson, et al. 2009. Interferometric fluorescent super-resolution microscopy resolves 3D cellular ultrastructure. *Proc. Natl. Acad. Sci. USA*. 106:3125–3130. doi:10.1073/pnas.0813131106
- Sieber, J.J., K.I. Willig, R. Heintzmann, S.W. Hell, and T. Lang. 2006. The SNARE motif is essential for the formation of syntaxin clusters in the plasma membrane. *Biophys. J.* 90:2843–2851. doi:10.1529/biophysj.105.079574
- Staudt, T., M.C. Lang, R. Medda, J. Engelhardt, and S.W. Hell. 2007. 2,2'-thiodiethanol: a new water soluble mounting medium for high resolution optical microscopy. *Microsc. Res. Tech.* 70:1–9. doi:10.1002/jemt.20396
- Steinhauer, C., C. Forthmann, J. Vogelsang, and P. Tinnefeld. 2008. Super-resolution microscopy on the basis of engineered dark states. *J. Am. Chem. Soc.* 130:16840–16841. doi:10.1021/ja806590m
- Subach, F.V., G.H. Patterson, S. Manley, J.M. Gillette, J. Lippincott-Schwartz, and V.V. Verkhusha. 2009. Photoactivatable mCherry for high-resolution two-color fluorescence microscopy. *Nat. Methods*. 6:153–159. doi:10.1038/nmeth.1298
- van de Linde, S., U. Endesfelder, A. Mukherjee, M. Schüttelpelz, G. Wiebusch, S. Manley, M. Heilemann, and M. Sauer. 2009. Multicolor photoswitching microscopy for subdiffraction-resolution fluorescence imaging. *Photochem. Photobiol. Sci.* 8:465–469. doi:10.1039/b822533h
- van Zanten, T.S., A. Cambi, M. Koopman, B. Joosten, C.G. Figdor, and M.F. Garcia-Parajo. 2009. Hotspots of GPI-anchored proteins and integrin nanoclusters function as nucleation sites for cell adhesion. *Proc. Natl. Acad. Sci. USA*. 106:18557–18562. doi:10.1073/pnas.0905217106
- Verveer, P.J., J. Swoger, F. Pampaloni, K. Greger, M. Marcelllo, and E.H. Stelzer. 2007. High-resolution three-dimensional imaging of large specimens with light sheet-based microscopy. *Nat. Methods*. 4:311–313.
- Vogelsang, J., R. Kasper, C. Steinhauer, B. Person, M. Heilemann, M. Sauer, and P. Tinnefeld. 2008. A reducing and oxidizing system minimizes photobleaching and blinking of fluorescent dyes. *Angew. Chem. Int. Ed. Engl.* 47:5465–5469. doi:10.1002/anie.200801518
- Wallace, W., L.H. Schaefer, and J.R. Swedlow. 2001. A workingperson's guide to deconvolution in light microscopy. *Biotechniques*. 31:1076–1078. doi:10.1002/biot.1082
- Westphal, V., S.O. Rizzoli, M.A. Lauterbach, D. Kamin, R. Jahn, and S.W. Hell. 2008. Video-rate far-field optical nanoscopy dissects synaptic vesicle movement. *Science*. 320:246–249. doi:10.1126/science.1154228
- Wicker, K., S. Sindbert, and R. Heintzmann. 2009. Characterisation of a resolution enhancing image inversion interferometer. *Opt. Express*. 17:15491–15501. doi:10.1364/OE.17.015491
- Willig, K.I., S.O. Rizzoli, V. Westphal, R. Jahn, and S.W. Hell. 2006. STED microscopy reveals that synaptotagmin remains clustered after synaptic vesicle exocytosis. *Nature*. 440:935–939. doi:10.1038/nature04592
- Willig, K.I., B. Harke, R. Medda, and S.W. Hell. 2007. STED microscopy with continuous wave beams. *Nat. Methods*. 4:915–918. doi:10.1038/nmeth1108
- Wilson, T., M.A. Neil, and R. Juskaitis. 1998. Real-time three-dimensional imaging of macroscopic structures. *J. Microsc.* 191:116–118. doi:10.1046/j.1365-2818.1998.00403.x